ELSEVIER

Journal of Alloys and Compounds 469 (2009) 458–463

Journal of ALLOYS AND COMPOUNDS

www.elsevier.com/locate/jallcom

Influences of deposition time and pH on magnetic NiFe nanowires fabrication

Funda Ersoy Atalay [a,*], Harun Kaya [a], Selçuk Atalay [a], Süleyman Tari [b]

[a] *Inonu University, Science and Art Faculty, Department of Physics, Malatya 44280, Turkey*
[b] *Science Faculty, Department of Physics, IYTE, İZMİR, Turkey*

Received 29 October 2007; received in revised form 30 January 2008; accepted 30 January 2008
Available online 14 March 2008

Abstract

In this work, NiFe nanowires were grown into highly ordered porous anodic alumina oxide (AAO) templates by dc electrodeposition at various deposition times and pH values. During the deposition process some electrochemical bath parameters such as ion content, deposition voltage, and temperature of solution were kept constant. The morphological properties of the nanowire arrays were studied by scanning electron microscopy (SEM) and transmission electron microscopy (TEM), the chemical composition was determined by examination of the energy dispersive X-ray (EDX) spectra, and the magnetic behavior of the arrays was determined by vibrating sample magnetometer (VSM).

PACS: 81.15.Pq; 62.23. Hj; 75.75.+a

Keywords: Nanopores; NiFe nanowires; Electrodeposition; Magnetic properties; pH

1. Introduction

There has been an explosive growth of nanoscience and nanotechnology in the last few years, primarily because of the availability of new strategies for the synthesis of nanomaterials and new tools for characterization and manipulation [1]. It has been reported that low-dimensional nanoscale materials, which have a large surface area and possible quantum confinement effects, exhibit distinct optical, chemical and thermal properties [2]. Much progress has been made in the preparation of low-dimensional nanomaterials by conventional lithography combined with techniques such as molecular beam epitaxy [3–5] and chemical vapor deposition [6]. However, lithographic techniques have some technological and economic limitations in the fabrication of ordered high-density nanoarrays. Template synthesis based on ordered anodic aluminum oxide (AAO) has attracted much interest because of the wide application in fabricating nanodot, nanowire and nanotube arrays [1–9]. So far, Ni, Fe and Co nanowires have been produced in ordered Al_2O_3 substrates with template synthesis methods, and their electrical and magnetic properties have been studied [9–15]. Permalloy is used extensively in the construction of magnetic recording heads, inductors and microrelays [16–20]. The mechanism of permalloy electrodeposition has been studied widely, but the production of nanowires of permalloys with various deposition times has not been investigated in detail.

Here, we have produced self-assembled arrays of NiFe nanowires in an AAO template with various deposition times.

2. Experimental details

The following procedure was used to synthesize AAO templates and magnetic nanowires inside them. The AAO templates were prepared by the conventional two-step anodic oxidation procedure [21] as shown in Fig. 1. Aluminum foil (99.99% purity) was used as the anode with an exposed area of 1 cm^2. The Al foil was cleaned with HCl, rinsed with distilled water and acetone, and then annealed at 500 °C for 2 h. The first anodization was performed in 0.3 M oxalic acid at various constant anodizing voltages (30–200 V) at room temperature. The template was immersed in a mixture of 6.0 wt.% H_3PO_4 and 1.8 wt.% H_2CrO_4 at room temperature to remove alumina. A second anodic oxidation and wet etching was done under the first-step conditions. Any remaining Al was removed with saturated $HgCl_2$. Different times of anodic oxidation and wet etching were investigated to find conditions suitable for the production of ordered high-density nanopores of various diameters.

A three-electrode cell was used for the electrochemical experiments. The volume of the electrochemical bath was approximately 85 ml. An Ag/AgCl

* Corresponding author. Tel.: +90 4223410010; fax: +90 4223410037.
E-mail address: fatalay@inonu.edu.tr (F.E. Atalay).

0925-8388/$ – see front matter © 2008 Elsevier B.V. All rights reserved.
doi:10.1016/j.jallcom.2008.01.141

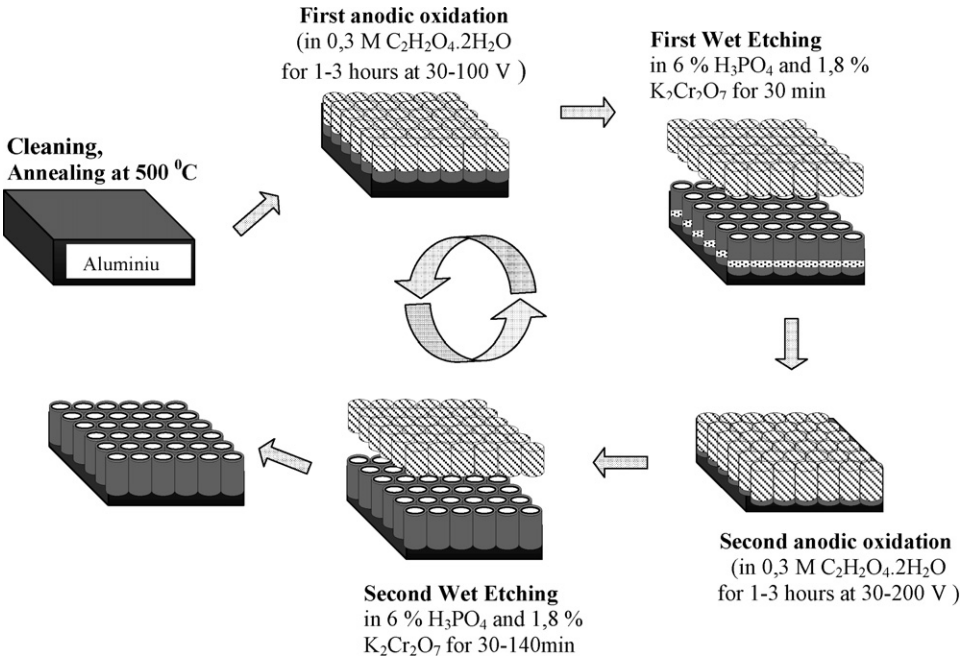

Fig. 1. A representation of the anodic oxidation process.

electrode (BAS, 3 M NaCl, and −35 mV versus SCE at 25 °C) was used as the reference electrode. AAO templates with approximately 200 nm diameter pores were coated with Au/Pd to a thickness of 5 nm. These templates were used as the cathode with an exposed area of approximately 1 cm^2. A platinum electrode approximately 5 times larger than the cathode was used as an auxiliary electrode. The bath contents are given in Table 1. All solutions were prepared by dissolving reagent-grade chemicals in distilled water. The bath pH was adjusted to the required value by adding 0.1 mM HCl or 0.1 mM NaOH monitored with a Jenway 3520 pH meter. The deposition was performed for 30–230 min to produce nanowires of various lengths. The electrodeposition was controlled by computer-controlled electrochemical workstation made in-house [22].

The morphology of the templates and nanowire arrays was investigated by scanning electron microscopy (SEM; LEO-EVO-40 instrument). The quantitative chemical analyses of the alloys were performed by energy dispersive X-ray (EDX) spectroscopy. Magnetic measurements of the arrays as a whole were performed with a vibrating sample magnetometer (VSM; Lake Shore 7407).

Table 1
Bath contents and electrodeposition conditions for production of NiFe nanowires

Chemicals	Concentration
$Ni(SO_4)_2{\cdot}6H_2O$	0.1 M
$Fe(SO_4)_2{\cdot}7H_2O$	5 mM
H_3BO_3	0.2 M
NaCl	35 mM
Saccharin	7 mM
Sodium lauryl sulfate	0.1 g/l
Operating conditions	
Bath pH	2, 2.6
Bath temperature	Room temperature
Deposition duration	30–230 min
Deposition potential	−2 V vs. Ag/AgCl
Agitation paddle	5 cycles/s

3. Results and discussion

The anodic oxidation steps and wet etching conditions determine characteristics of the array such as pore diameter, interpore distance and ordering degree of pores, and length of the nanopores. It was found that the applied voltage could control pore size as well as pore separation, as reported [23,24]. Fig. 2 shows SEM images of ordered porous anodic alumina for 30, 40 and 100 V anodic oxidation voltages, and it is clear that pore diameter increases with increasing anodizing voltage. An

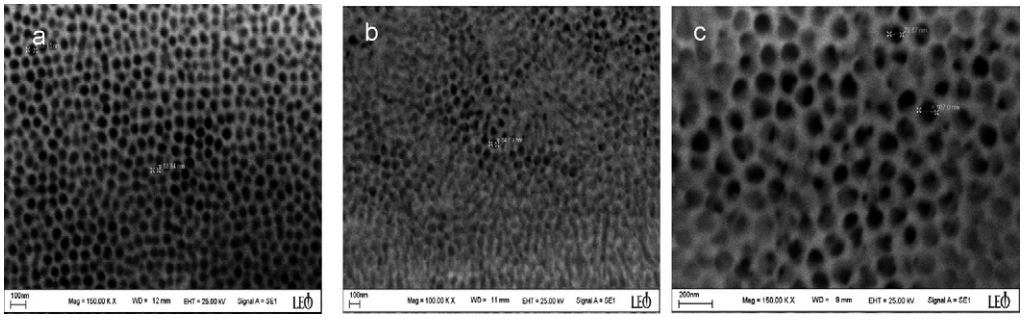

Fig. 2. SEM images of ordered nanopore arrays prepared by two-step anodic oxidation conducted at different anodic oxidation potentials: (a) 30 V; (b) 40 V; (c) 100 V. The second etching time was 100 min.

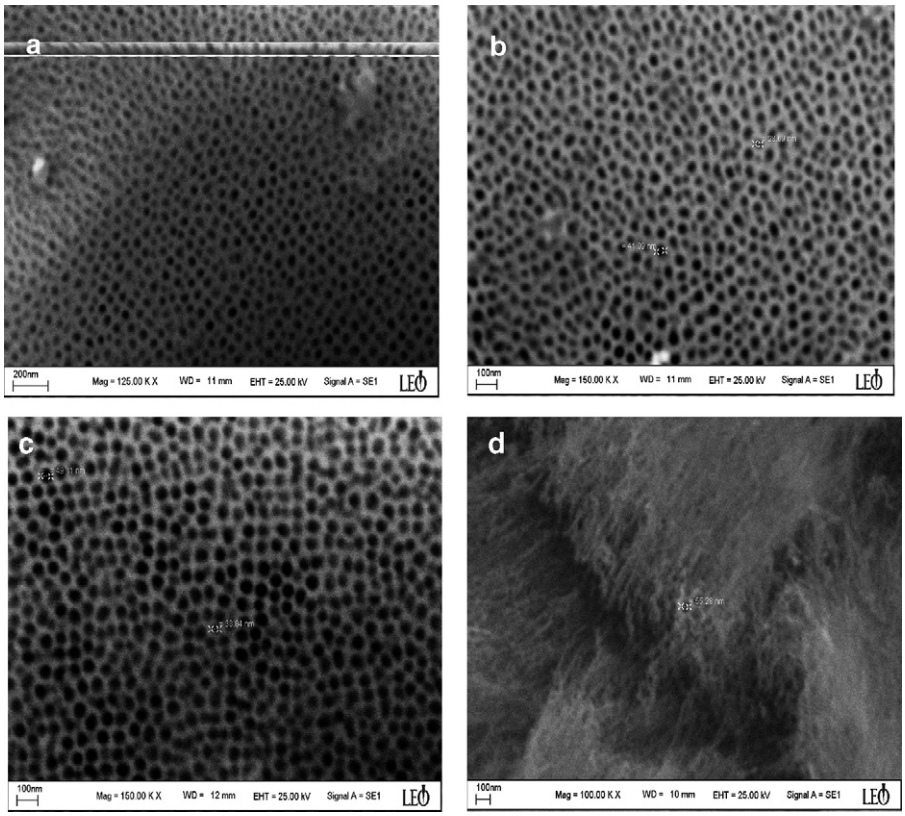

Fig. 3. SEM images of ordered nanopore arrays prepared by two-step anodic oxidation (3 h + 1 h) at 30 V for different second etching times: (a) 5 min, (b) 25 min, (c) 40 min, and (d) 140 min.

average pore diameter of 35–50 nm was obtained for anodic oxidation at 30 V (Fig. 2a). When the second wet etching time was 100 min, the average pore size was approximately 50–65 nm for 40 V and 75–105 nm for 100 V, as shown in Fig. 2b and c.

It can be seen from Fig. 3 that pore size increases with increasing time of the second wet etching with constant anodic oxidation at 30 V: a typical pore diameter was about 30–40 nm for 25 min (Fig. 3b) and 40–50 nm for 40 min (Fig. 3c). After second etching for 140 min, the ordered porous structure was *destroyed* as shown in Fig. 3d. It was noted also that the anodic oxidization procedure leads to homogeneous pore density on the template.

The amount of electrochemical reaction at the cathode is proportional to the quantity of electric charge (Q) passed through the Au/Al_2O_3 template. It follows that the thickness of the electrodeposited layer will be proportional to the deposition time when the other plating parameters, such as plating voltage and pH, are constant. The deposition time was varied from 30 to 230 min to produce NiFe nanowires with different lengths on the Al_2O_3 template.

Fig. 4 shows the current behavior as a function of pH during the deposition of nanowires. Electrodeposition curves were obtained in a stirred electrolyte at a constant potential of −2 V versus Ag/AgCl. The current versus time plot shows that growth of the nanowires was often not a steady-state process, and it appears that there was significant current oscillation as voltage was applied to the cathode. The current increased suddenly when the pores were empty, and dropped gradually with filling of the pores at pH 2, but there was a broad peak overlapping the decaying current at pH 2.6. In our previous works [25–27], we observed that electrodeposited NiFe average grain sizes and thickness of the plated layer were smaller at low pH values than at high pH values. Thus, it can be assumed that the process of nanowires filling the pores occurred slowly at pH 2.6.

As already reported [18,19,28,29], at the first stage of current–time transient curve (Fig. 4), the porous deposition is

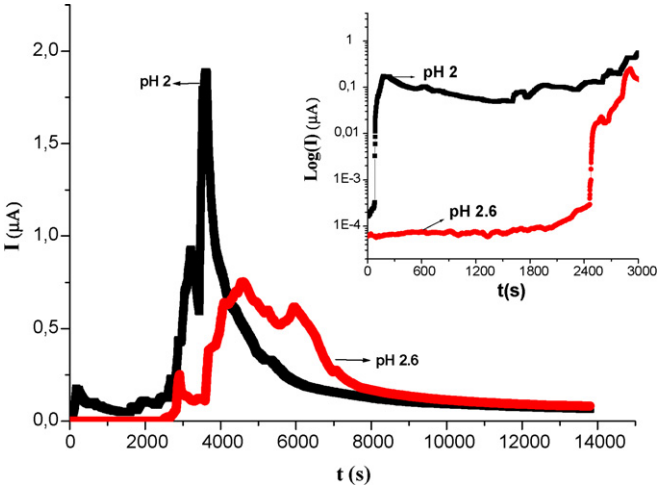

Fig. 4. Current transients curve of NiFe electrodeposition solution at −2 V constant deposition potential for 230 min vs. Ag/AgCl. Inset shows low deposition time region.

believed to be due to the side reactions occurring in the metal deposition. Firstly, hydrogen from the side reactions may be included in the deposit. Secondly, metal hydroxide can precipitate at a high pH resulting from the side reactions. This 'crispy' part of the deposit is weak and cannot be sustained during electrodeposition. This effect is apparently reflected as a fluctuation in current transient curves at first 60 min.

The average composition of the alloy nanowires was evaluated by EDX microanalysis (Fig. 5). The NiFe nanowire sample electrodeposited at pH 2 for 120 min showed a Ni/Fe ratio of 72:28. The sample deposited at pH 2.6 for 230 min had a Ni/Fe ratio of 79:21. The increase of the Ni/Fe ratio with increasing deposition time for both pH values is shown in Fig. 6. The variation of the alloy composition with deposition parameters can be explained by well-known anomalous codeposition effect in permalloys [30]. Among the hypotheses found in literature to explain this anomaly [31–35], the most wide spread one, is the so-called 'hydroxide suppression mechanism' (HSM) [33–35]. This model, initially proposed by Dahms and Croll [32] for the NiFe system, suggests that the precipitation of a less noble metal hydroxide at the cathode is able to inhibit the deposition of the more noble metal. Based on this theory, deposition conditions that can cause surface pH increase would enhance the anomalous codeposition [33–35]. The abrupt increase of current after

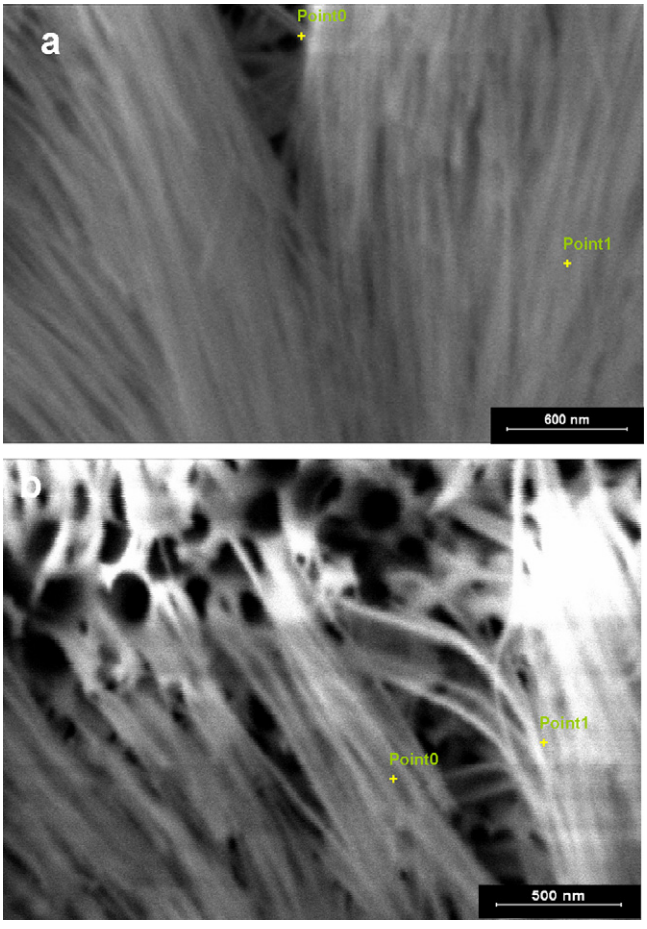

Fig. 5. EDX point analysis for NiFe nanowire arrays electrodeposited at −2 V for (a) pH 2 for 120 min and (b) pH 2.6 for 230 min.

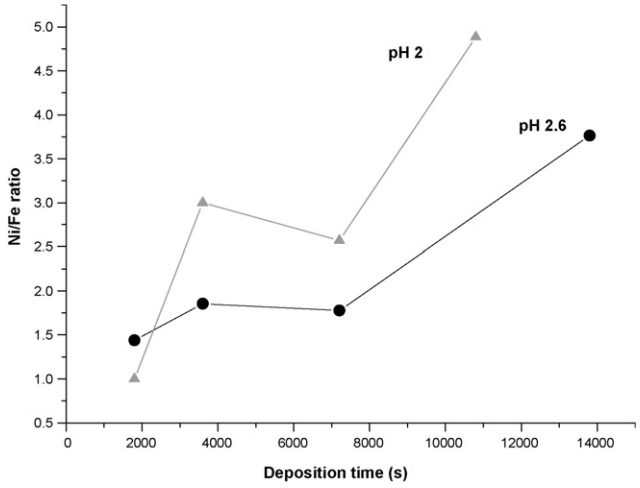

Fig. 6. NiFe ratio vs. deposition time obtained by EDX analysis.

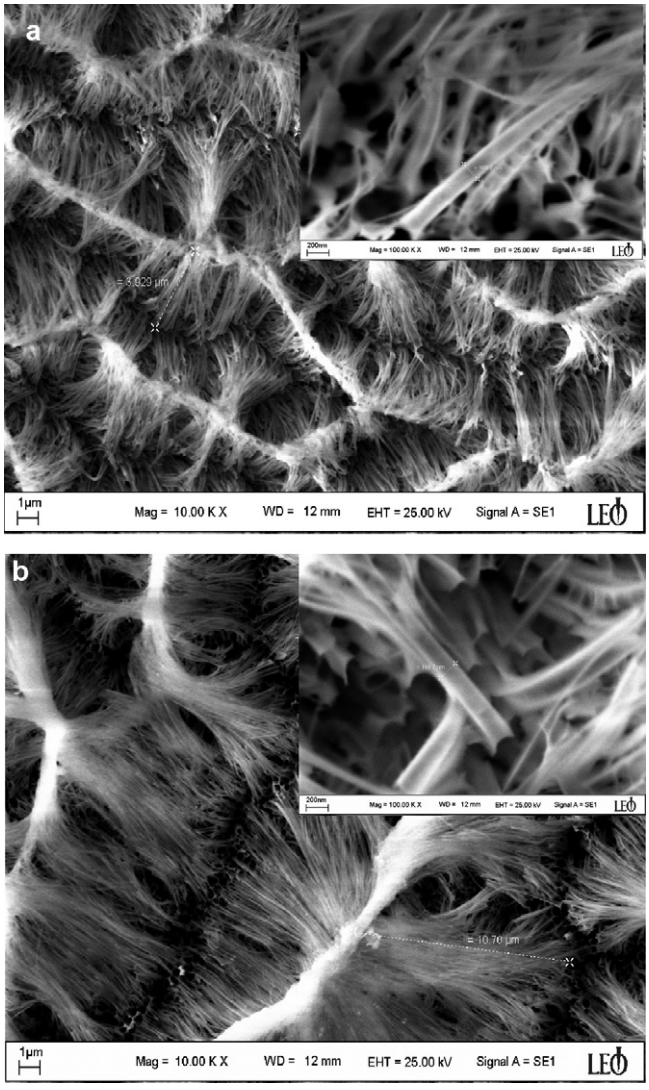

Fig. 7. SEM images of ordered NiFe nanowire arrays electrodeposited at pH 2 after etching in 1 M NaOH for 5 min. The deposition time was (a) 30 min, and (b) 120 min. The insets are SEM images of the Ni–Fe nanowires taken at a higher magnification.

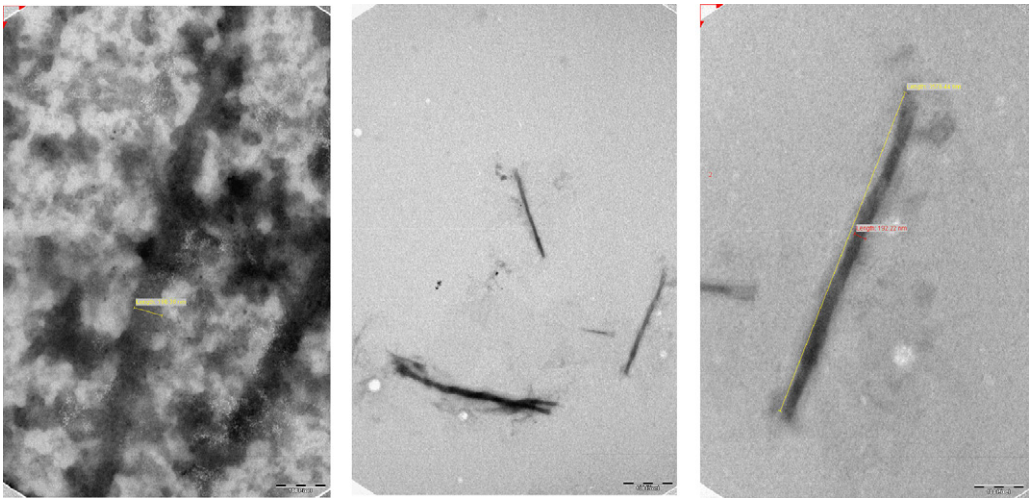

Fig. 8. TEM images of electrodeposited NiFe nanowires.

60 min in Fig. 4 is connected with depletion of Fe species by diffusion. By increasing the deposition time, anomalous of Ni and Fe electrodeposition was established, which allow the increase at the Ni/Fe ratio for obtaining the composition of $Ni_{80}Fe_{20}$. A steady-state value of high current was reached after 230 min, which corresponds to the filling of the pores.

The morphology of the NiFe nanowires obtained in the pores of the Al_2O_3 template is shown in Fig. 7, after the partial dissolution of the membrane in 1 M NaOH for 30 min and for 120 min of deposition. A clear morphological elongation was observed in the electrodeposited nanowires as a function of deposition time. The length of the nanowires was approximately 4–5 and 8–10 μm with deposition times of 30 and 120 min, respectively (Fig. 7a and b). The nanowires deposited inside the nanopores of the AAO template are parallel, aligned regularly and densely distributed. The average diameter of the nanowires corresponded closely to a pore diameter of 185–195 nm. This result was supported by transmission electron microscope (TEM) images of NiFe nanowires electrodeposited for 30 min (Fig. 8). For the TEM images, the sample was kept in NaOH, to remove the AAO template, dissolve the alumina and liberate the nanowires, which were then suspended in hexane. It was observed clearly that the duration of deposition affects the length of the nanowires but not the diameter.

The reduced hysteresis curves of the NiFe nanowire arrays obtained with the AAO template are shown in Fig. 9. It is observed from the reduced hysteresis curves, that the magnetic behavior of the NiFe nanowire arrays was strongly dependent on

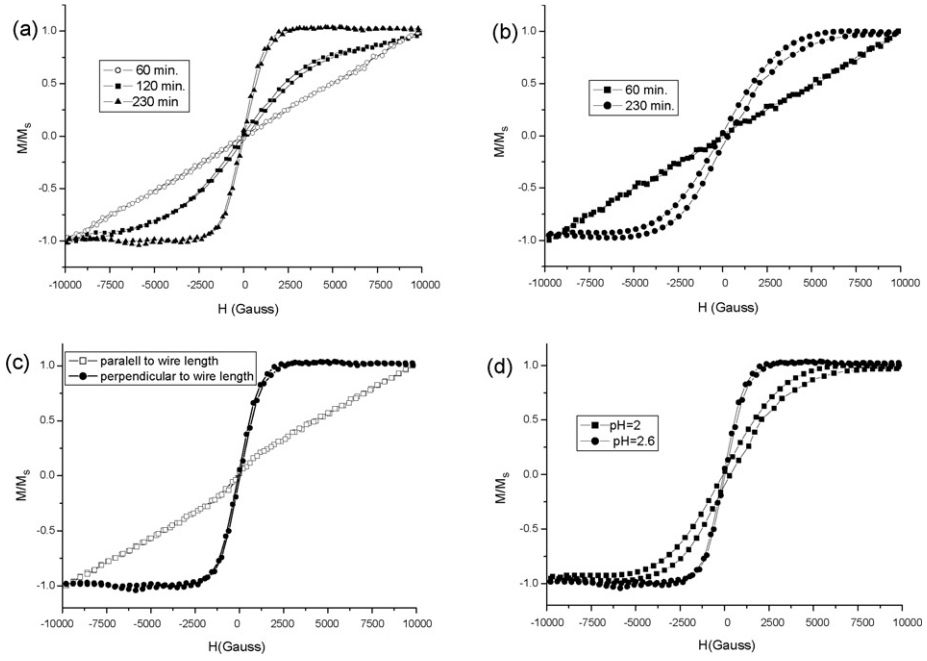

Fig. 9. Magnetic hysteresis loops of NiFe nanowire arrays. (a) Nanowires deposited for various times at pH 2.6, magnetic field is applied to parallel to wire length. (b) Nanowires deposited for various times at pH 2, magnetic field is applied to parallel to wire length. (c) Magnetization loops of 230 min deposited wire at pH 2.6. (d) Nanowires deposited for 230 min at pH 2 and 2.6; magnetic field is applied to parallel to wire length.

deposition time and pH of solution. The coercivities of the NiFe nanowire arrays obtained in the AAO template with a deposition time of 230 min at pH 2.6 were 90 and 71 G for the applied field perpendicular to and parallel with the nanowire arrays, respectively. The magnetization loops of the 60 and 120 min deposited wires could not reach the saturation at 10 kG. The magnetization loops of nanowire arrays deposited for 60 and 120 min at pH 2.6 showed perpendicular anisotropy, which could be a consequence of the geometry of the nanowire arrays [36]. Fig. 9 also indicates that the magnetic anisotropy decreases with the increasing deposition time. Assuming that nanowires are in the shape of a uniform cylinder, when the sample length increases with the increasing deposition time, the demagnetization factor and therefore demagnetization energy decreases leading to a decrease in the total magnetic anisotropy.

It can be seen that the nanowire arrays deposited for 230 min at pH 2 and 2.6 were saturated when the magnetic field applied along the length of the nanowires. In contrast, when the field was applied perpendicular to the nanowires, the magnetization did not reach saturation at a magnetic field of 10 kG. That is to say, the easy axis of magnetization of nanowires deposited over 230 min at pH 2.6 is close to the long axis of the nanowires. It was found that the nanowires produced at pH 2.6 have softer magnetic properties than the samples produced at pH 2 (Fig. 9d). The comparison of Fig. 6 with Fig. 9 clearly indicate that there is a relation between time dependence of composition with the shape of magnetization loops, where the increase of Ni content could be partly the cause for the increase of permeability.

4. Conclusion

Ordered NiFe nanowire arrays were produced by electrodeposition with AAO as the template. SEM observations indicate that ordered NiFe nanowire arrays are parallel, regularly aligned and densely distributed within the AAO template. The magnetic properties of nanowire arrays can be improved by optimizing the deposition time and pH of the solution. It was found that the nanowires produced at pH 2.6 have softer magnetic properties than the samples produced at pH 2.

Acknowledgment

This work was supported by TUBITAK with Project number TBAG-105T459.

References

[1] C.N.R. Rao, A. Müler, A.A.K. Cheetham, The Chemistry of Nanomaterials, WILEY-VCH, Weinheim, 2004.
[2] M. Law, J. Goldberger, P. Yang, Ann. Rev. Mater. Res. 34 (2004) 83.
[3] M.A. McCord, M.J. Rooks, in: P. Rai-Choudhury (Ed.), Handbook of Microlithography, Micromachining and Microfabrication, SPIE Press, IEEE, 1999, pp. 139–250.
[4] C.M. Sotomayor Torresa, S. Zankovycha, J. Seekampa, A.P. Kama, C. Clavijo Cedenoa, T. Hoffmanna, J. Ahopeltob, F. Reutherc, K. Pfeifferc, G. Bleidiesselc, G. Gruetznerc, M.V. Maximovd, B. Heidarie, Mater. Sci. Eng. C 23 (2003) 23.
[5] R. Krahne, A. Yacoby, H. Shtrikman, I. Bar-Joseph, T. Dadosh, J. Sperling, Appl. Phys. Lett. 81 (2002) 730.
[6] H. Chik, J.M. Xu, Mater. Sci. Eng. R 43 (2004) 103.
[7] H.X. He, N.J. Tao, in: N.S. Nalwa (Ed.), Encyclopedia of Nanoscience and Nanotechnology, American Scientific Publishers, 2004, pp. 755–772.
[8] M.T. Wu, I.C. Leu, J.H. Yen, M.H. Hon, Electrochem. Solid-State Lett. 7 (2004) C61.
[9] D.J. Sellmyer, M. Zheng, R. Skomski, J. Phys.: Condens. Matter 13 (2001) R433.
[10] P.R. Evans, G. Yi, W. Schwarzacher, Appl. Phys. Lett. 76 (2000) 481.
[11] H. Pan, B. Liu, J. Yi, C. Poh, S. Lim, J. Ding, Y. Feng, C.H.A. Huan, J. Lin, J. Phys. Chem. B 109 (2005) 3094.
[12] X.W. Wang, G.T. Fei, X.J. Xu, Z. Jin, L.D. Zhang, J. Phys. Chem. B 109 (2005) 24326.
[13] X.Y. Zhang, L.H. Xu, J.Y. Dai, H.L.W. Chan, Physica B 353 (2004) 187.
[14] C.Z. Wang, G.W. Meng, Q.Q. Fang, X.S. Peng, Y.W. Wang, Q. Fang, L.D. Zhang, J. Phys. D: Appl. Phys. 35 (2002) 738.
[15] A. Saedi, M. Ghorbani, Mater. Chem. Phys. 91 (2005) 417.
[16] A.G. Munoz, C. Schiefer, Th. Nentwig, W.-Y. Man, E. Kisker, J. Phys. D: Appl. Phys. 40 (2007) 5013.
[17] J.O'M. Bockris, D. Drazic, A.R. Despic, Electrochim. Acta 4 (1961) 325.
[18] D. Gangasingh, J.B. Talbot, J. Electrochem. Soc. 138 (1991) 3605.
[19] J.M. Quemper, S. Nicolas, J.P. Gilles, J.P. Grandchamp, A. Bosseboeuf, T. Bourouina, E. Dufour-Gergam, Sens. Actuators 74 (1999) 1.
[20] T. Osaka, Electrochim. Acta 45 (2000) 3311.
[21] H. Masuda, K. Fukuda, Science 268 (1995) 1466.
[22] F.E. Atalay, M.Sc. Thesis, Inonu University, Malatya, Turkey, 1994.
[23] S. Ono, M. Saito, M. Ishiguro, H. Asoh, J. Electrochem. Soc. 151 (2004) B473.
[24] X. Peng, A. Chen, Nanotechnology 15 (2004) 743.
[25] H. Kaya, M.Sc. Thesis, Inonu University, Malatya, Turkey, 2005.
[26] F.E. Atalay, H. Kaya, S. Atalay, Physica B 371 (2006) 327.
[27] F.E. Atalay, S. Atalay, J. Alloys Compd. 392 (2005) 322.
[28] A.G. Muñoz, D.R. Salinas, J.B. Bessone, Thin Film Solids 429 (2003) 119–128.
[29] N. Zech, E.J. Podlaha, D. Landolt, J. Electrochem. Soc. 146 (1999).
[30] A. Brenner, Electrodeposition of Alloys, vol. I, Academic Press, 1962, 77 pp.
[31] M.J. Nicol, H.I. Philip, J. Electroanal. Chem. 70 (1976) 233.
[32] H. Dahms, I.M. Croll, J. Electrochem. Soc. 112 (1965) 771.
[33] H. Fukushima, T. Akiyama, M. Yano, T. Ishikawa, R. Kammel, ISIJ Int. 33 (1993) 1009.
[34] T. Akiyama, H. Fukushima, ISIJ Int. 32 (1992) 787.
[35] H. Fukushima, T. Akiyama, K. Higashi, R. Kammel, M. Karimkhani, Metallurgy 44 (1990) 754.
[36] C.-L. Xu, H. Li, G.-Y. Zhao, H.-L. Li, Mater. Lett. 6 (2006) 2335.